Review

Israel Journal of Chemistry

DOI: 10.1002/ijch.201400146

Sculpting Metal-binding Environments in *De Novo* Designed Three-helix Bundles

Jefferson S. Plegaria and Vincent L. Pecoraro*[a]

Abstract: *De novo* protein design is a biologically relevant approach used to study the active centers of native metalloproteins. In this review, we will first discuss the design process in achieving α_3D, a *de novo* designed three-helix bundle peptide with a well-defined fold. We will then cover our recent work in functionalizing the α_3D framework by incorporating a tris(cysteine) and tris(histidine) motif. Our first design contains the thiol-rich sites found in metalloregulatory proteins that control the levels of toxic metal ions (Hg, Cd, and Pb). The latter design recapitulates the catalytic site and activity of a natural metalloenzyme carbonic anhydrase. The review will conclude with future design goals aimed at introducing an asymmetric metal-binding site in the α_3D framework.

Keywords: protein design · metal ions · metalloproteins · three-helix bundles · three-stranded coiled-coils

1. Introduction

Proteins acquire metal ions, such as iron, copper, or zinc, to perform essential functions in biology, including catalytic reactions, signal transduction, transport and storage of small molecules, and redox chemistry.[1] Metalloproteins play a central role in various biological systems, including photosynthesis and respiration, two systems that sustain all life on earth. Recent initiatives by the scientific community to find alternatives to carbon-based fuels have turned to the bioenergetic processes in photosynthesis for inspiration to create a "greener planet". Before efficient artificial photosynthetic systems can be realized, fundamental research on the individual metalloproteins and metalloenzymes in this multifaceted system must be explored. Ultimately, the knowledge gained from this research will bring us one step closer to fully understanding and harvesting the rewards of many biological systems.

Protein design is a biologically relevant approach used to study the concept of the structure-function relationship in native proteins.[2–4] This emerging approach has two central design strategies: the first is protein redesign,[2] and the second is *de novo* design.[2–7] Protein redesign involves modifying or incorporating the desired metal-binding site in an existing native protein scaffold. The second approach, which is unquestionably the most challenging strategy, employs first principles to design peptide or protein scaffolds from scratch, with an amino acid sequence not found in nature.[6] It allows one to tailor-design a sequence that forms the proper hydrophobic, electrostatic, and hydrogen-bonding interactions that will manifest into a well-defined peptide scaffold, an important characteristic of native proteins. *De novo* protein design offers a novel approach in studying the mechanisms behind protein folding and exploring the active sites of native proteins in a simplified or unrelated fold. The knowledge gained from this approach could ultimately provide insight into the fundamental processes of biological systems, thus allowing the possibility of producing new metalloproteins, with higher stability and superior efficiency than native proteins, for many biotechnological applications.

We are actively involved in the *de novo* protein design of peptide scaffolds to understand the metal active sites of metalloenzymes (Figure 1a), as well as metalloproteins involved in electron transfer (ET, Figure 1b), metal-regulated gene expression,[1,8] and metallochaperones.[1] These last systems are a subset of metalloproteins used by microorganisms to control the levels of essential transition metal ions (Fe, Cu, Zn, and Mn), decrease levels of toxic metals (Hg, As, Pb, and Cd) within their cells, and to ensure proper trafficking and insertion of metals into enzymes or secretory vesicles. This review focuses on a *de novo* designed scaffold, α_3D,[9] a single polypeptide chain that folds into a three-helix bundle (THB). Section 2 will first briefly cover our work and progress with three-stranded coiled-coil (3SCC) constructs. It will then be followed by the achievement of DeGrado and coworkers in producing a THB scaffold. Next, section 3 will cover our

[a] J. S. Plegaria, V. L. Pecoraro
930 North University Ave
Department of Chemistry
University of Michigan
Ann Arbor, Michigan 48109 (USA)
Tel: (+1) 734-763-1519
e-mail: vlpec@umich.edu

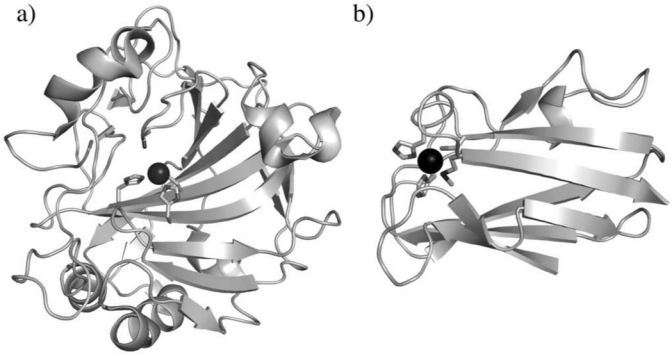

Figure 1. a) Crystal structure of a zinc metalloenzyme, human carbonic anhydrase II (PDB code 3KS3).[12] b) Crystal structure of a copper electron-transfer metalloprotein, plastocyanin (PDB code 1PLC),[13] which is part of the cupredoxin family.

current work and first approach in functionalizing the α_3D scaffold through the incorporation of symmetric metal-binding sites to yield peptides α_3D**IV**[10] and α_3D$\mathbf{H_3}$.[11] Our work comprises a short description of the solution structure of α_3D**IV** (unpublished work), an α_3D analogue that contains a tris(cysteine) motif, and its heavy metal binding properties. In addition, we will also describe our progress with a carbonic anhydrase model, α_3D$\mathbf{H_3}$, an iteration of α_3D that contains a tris(histidine) site. The last section will discuss future designs that aim to improve metal binding in α_3D**IV** and catalytic activity in α_3D$\mathbf{H_3}$, as well as to model an asymmetric $His_2CysMet$ copper site.

Vincent L. Pecoraro is the John T. Groves Collegiate Professor of Chemistry at the University of Michigan. His research group is deeply involved in *de novo* metalloprotein design and metallamacrocyclic chemistry. Prof. Pecoraro has received numerous awards and honors, including the G. D. Searle Biomedical Research Scholarship, an Alfred P. Sloan Fellowship, the Vanadis Award, an Alexander von Humboldt Award for Senior Research Scientists, and The Blaise Pascal International Chair for Research. He is a Fellow of the American Association for the Advancement of Science and the American Chemical Society. He has served as an Associate Editor of Inorganic Chemistry since 1994.

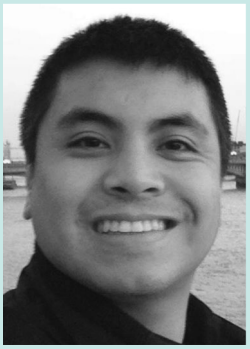

Jefferson S. Plegaria received his B.A. degree in Chemistry from La Salle University, Philadelphia, PA, in 2007. He then worked in the pediatric-oncology lab of Dr. John Maris at The Children's Hospital of Philadelphia. In 2009, he began his Ph.D. degree with Professor Vincent L. Pecoraro. He is currently studying the spectroscopic and electron-transfer properties of *de novo* designed cupredoxin models using biophysical, electrochemical, and photophysical methods.

2. Development of *De Novo* Designed Scaffolds

2.1. Three-stranded Coiled-coil Constructs

The most common *de novo* designed peptides use a heptad repeat sequence (abcdefg) that self-assemble into a parallel 3SCC tertiary structure (Figure 2a).[7,14,15]

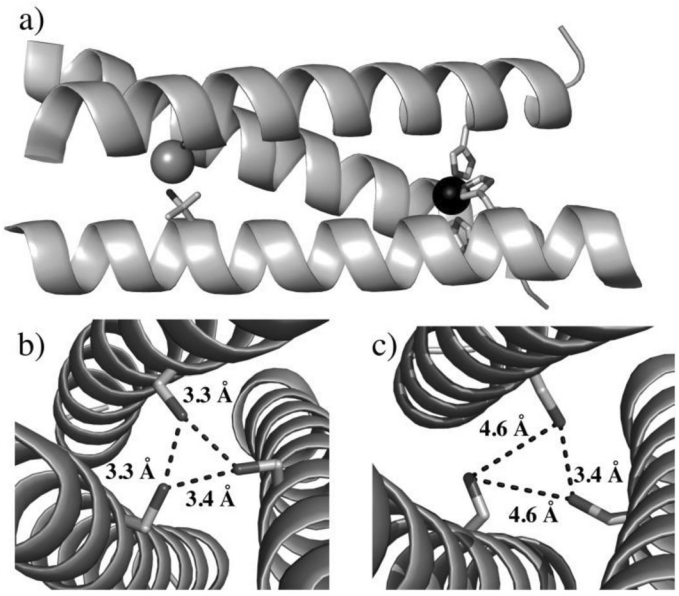

Figure 2. a) Crystal structure of $[Hg(II)]_S[Zn(II)(H_2O/OH^-)]_N$-$(CSL9PenL23H)_3^{n+}$ (PDB code 3PBJ), which is used as a crystallographic model for the $[Hg(II)]_S[Zn(II)(H_2O/OH^-)]_N(TRIL9CL23H)_3^{n+}$ CA model.[27, 30] This bimetallic 3SCC construct contains a Zn(II) and Hg(II) atom bound to a His-N_3 and Pen-S_3 site, respectively. b) Symmetric "a" site Cys residues in CSL9C (PDB code 3LJM)[37] contain Sγ ligands that orient inside the core. c) Symmetric "d" site Cys residues in CSL19C (PDB code 2X6P)[37] include Sγ ligands that orient towards the interhelical interface, forming a larger metal-binding site than Cys "a" sites.

Much of our effort and success in the *de novo* design field has been carried out using the 3SCC scaffold of TRI,[16–31] Grand (Gr),[24,26,32,33] and BABY[18,33,34] peptides, as well as in CoilSer (CS),[22,27,28,33,35–37] which serves as a crystallographic analogue for TRI (Table 1). A metal-binding site is generated by incorporating a cysteine or penicillamine residue at the "a" (Figure 2b) or "d" (Figure 2c) position in a 3SCC scaffold.[37] We discovered that the subtle difference between the "a" and "d" positions can produce distinctive outcomes in heavy metal binding affinity and geometry, which can be attributed to the pre-organization of the sulfur ligands prior to metal bind-

Table 1. Amino acid sequence of *de novo* designed 3SCC analogues.[a]

Peptide	Sequence						
		abcdefg	**abcdefg**	**abcdefg**	**abcdefg**	**abcdefg**	
CoilSer	Ac-E	WEALEKK	LAALESK	LQALEKK	LEALEHG		$-NH_2$
Baby	Ac-G	LKALEEK	LKALEEK	LKALEEK			G-NH_2
TRI	Ac-G	LKALEEK	LKALEEK	LKALEEK	LKALEEK		G-NH_2
Grand	Ac-G	LKALEEK	LKALEEK	LKALEEK	LKALEEK	LKALEEK	G-NH_2

[a] Leucine residues at the "a" or "d" positions are mutated to metal-binding residues such as cysteine, penicillamine, or histidine. Mutation of Leu residues to Cys and His at the 9th and 23rd positions, respectively, is designated as TRIL9CL23H.

ing.[14,17] Overall, we have gained a deeper understanding in the metallobiochemistry of heavy metals, such as As(III),[19,28,35] Cd(II),[14,19–22,24–26,32] Hg(II),[16–19,22,23,25,27,34] and Pb(II),[21,28,33,38] in a tristhiolate site. We have demonstrated how to control the coordination number and geometry of Cd(II)[14,24,26,32] and Hg(II),[18,19,23,25] determined the affinity for Cd(II)[21] and Pb(II),[21,33] based on site preferences for "a" or "d" sites of the Cys residues, and elucidated the effects of the core aliphatic groups in the second coordination sphere on the molecular recognition of Cd(II)[14,24,26] and Pb(II).[33] This work on heavy metal chemistry in 3SCC is a culmination of over 10 years of research and has given us a solid foundation for modeling catalytic sites of natural metalloenzymes.

Using the 3SCC scaffold, our work has progressed into modeling the symmetric tris(histidine) metal-binding site found in carbonic anhydrase (CA)[27,30] and nitrite reductase (CuNiR).[29,31] The $[Hg(II)]_S[Zn(II)(H_2O/OH^-)]_N(TRIL9CL23H)_3^{n+}$ CA model (Figure 2a) of Zastrow *et al.* contains a structural $Hg(II)S_3$ site towards the N-terminal end of the TRI fold (Figure 3a) and a $Zn(II)N_3O$ catalytic site at the C-terminal end (Figure 3b).[27] This construct is an artificial metalloenzyme that catalyzes the hydration of CO_2 with an efficiency faster than any other small molecule model and is within ~500-fold of CAII, the most active isoform of carbonic anhydrase. Further, the CuNiR models of Tegoni *et al.*[29] and Yu *et al.*[31] are capable of multiple turnover catalysis for the one electron reduction of nitrite using ascorbate, and is the first mononuclear redox enzyme that was isolated via *de novo* protein design. Nevertheless, the metal-binding sites of native proteins, such as the ET site in cupredoxins, are often asymmetric and contain a mixed-ligand (O, N, or S) environment (Figure 3c).[13] Further, the coordination environment of metal centers contains secondary residues that participate in hydrogen-bonding networks (Figure 3c), such as in CA,[12,39] or in electrostatic interactions, which are essential in the catalytic or redox activity of many metalloproteins. Even though we have successfully modeled a variety of metal centers and performed catalytic reactions in our 3SCC scaffolds, its self-assembling nature makes it challenging to obtain asymmetric constructs. Therefore, to achieve asymmetric metal binding sites, we have expanded our work to acquire, and then later develop, a single polypeptide sequence that folds into a preformed three-helix bundle fold.

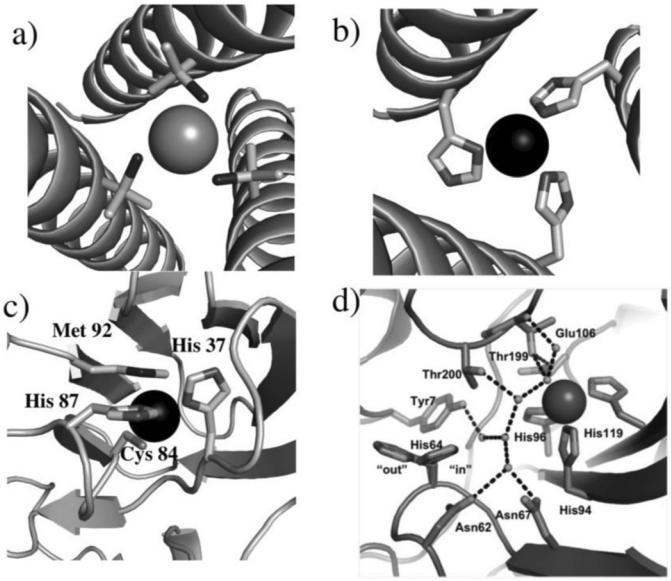

Figure 3. a) Top-down view of the trigonal $Hg(II)S_3$ site in $[Hg(II)]_S[Zn(II)(H_2O/OH^-)]_N(CSL9PenL23H)_3^{n+}$, which serves as a structural motif in the scaffold.[27] b) Top-down view of the $Zn(II)N_3O$ site in $[Hg(II)]_S[Zn(II)(H_2O/OH^-)]_N(CSL9PenL23H)_3^{n+}$, which is capable of CA activity.[27] c) 2His, Cys and Met copper binding site in plastocyanin, illustrating an asymmetric metal center.[13] d) Zinc metal-binding site in CAII, which contains a tris(histidine) site and hydrogen-bonding residues, such as Thr199, which are essential in catalysis.[12, 39] Reprinted with permission from Ref. [4]. Copyright 2014 American Chemical Society.

2.2. From Three-stranded Coiled-coil to a Three-helix Bundle Fold

The THB fold is used as a molecular recognition domain found in many biological systems including immunoglobulin G, DNA binding proteins, and various enzymes. Inspired by its universal presence and diverse function in nature, DeGrado and coworkers aimed to create a *de novo* designed antiparallel THB scaffold. Bryson *et al.* used the sequence of CS as the foundation, because its X-ray crystal structure[40] was observed to pack in an antiparallel manner, where the helices orient in an up-up-down manner, instead of the predicted parallel style.[41]

Table 2. Amino acid sequence of THB analogues.[a]

Peptide	Sequence				Design Purpose/Function
	abcdefg	**abcdefg**	**abcdef**	**loop**	
α_3A	**E**WEALEKK	L**N**ALESK	LQALEK	**G**	Iteration of CS
	NWEAL**K**K**E**	L**N**AL**K**S**E**	LQAL**K**K	**PG**	
	EWEALEKK	L**N**ALESK	LQALE**HG**		
α_3B	EWEALEKK	L**A**ALESK	LQALEK	G**G**	Iteration of α_3A
	NPDEW**A**ALKKE	L**A**ALKSE	LQALK	**GKG**	
	NPEWEALEKK	L**A**ALESK	LQALEHG		
α_3C	**S**W**AEFKER**	LAA**IK**S**R**	LQAL	GG	Iteration of α_3B
	SEAE**L**AA**FE**KE	**I**AA**FE**SE	LQA**Y**K	GKG	
	NPE**V**EAL**R**K**E**	**A**AA**IR**S**E**	LQA**YR**H**N**		
α_3D	**MG**SWAEFK**Q**R	LAAIK**T**R	LQAL	GGS	Molecular
	EAELAAFEKE	IAAFESE	LQAY	KGKG	recognition domain
	NPEVEALRKE	AAAIR**D**E	LQAYRHN		
α_3DIV	MGSWAEFKQR	LAAIKTR	**C**QAL	GGS	Heavy metal
	EAE**C**AAFEKE	IAAFESE	LQAY	KGKG	peptide
	NPEVEALRKE	AAAIRDE	**C**QAYRHN		Cd(II), Hg(II) and Pb(II)
α_3D**H$_3$**	MGSWAEFKQR	LAAIKTR	**H**QAL	GGS	Carbonic anhydrase
	EAE**H**AAFEKE	IAAFESE	LQAY	KGKG	
	NPEVEALRKE	AAAIRDE	**H**QAYRHN**GSGA**		model

[a] The sequences are prepared in heptads. Residues that are underlined and bolded were changed from the previous design. The α_3A was altered from the CS sequence.

Using a hierarchical approach, α_3D[9] was the final product and was isolated through a step-wise process (3 design rounds) of modifying helix-capping interactions which dictate the topology of the bundle, electrostatic interactions which orient the desired helix-helix pairing to avoid alternative states, and hydrophobic interactions to achieve a well-packed core.

In the first round, Bryson *et al.* shortened the sequence of CS by one heptad repeat to yield three 21-residue helices in α_3A (Table 2).[41] To achieve an antiparallel strand, Glu and Lys residues in helix 2 at the "e" and "g" positions were reversed from the original positions in CS. Next, two simple loops of Gly-Asn and Pro-Gly-Asn were incorporated between helix 1 and 2 and helix 2 and 3, respectively, to serve as hairpin loops. This motif is essential for directing the topology of the bundle, which can adopt clockwise or a counterclockwise orientation. α_3A was observed to form monomer/dimer/trimer species in solution, indicating that the hairpin loops were not successful in stabilizing intermolecular interactions. Round two designs were a direct response to these issues.

Sequence α_3B was designed to contain stronger helix stop signals to accurately direct the formation and conformation of the loops. This was achieved by lengthening residues in the loops and adding Asn residues as a helix stop signal in the form of helix capping boxes (Asn-Pro-Asp-Glu between helix 1 and 2 and Asn-Pro-Glu between helix 2 and 3). α_3B is monomeric in solution but still retains some characteristics of a molten globule, an undefined folded state with several energetically equal conformations.

Lastly, the final round of design focused on repacking the hydrophobic core, reordering the residues involved in interhelical electrostatic interactions, and further enhancing helix-capping interactions to prevent nonnative characteristics in α_3B. First, an Asn was replaced with a Ser as the helix-capping residue between helix 1 and 2. Next, the positions of the Lys and Glu residues were redesigned to force a counterclockwise topology in the bundle (Figure 4). The clockwise form was destabilized by careful placement of charged residues at the "e" and "g" positions. In helix 1, only positively (+) charged residues were placed both at the "e" and "g" positions; while in helix 3, negatively (−) charged residues were assigned in those corresponding sites. For helix 2, the "e" sites were given only − charged residues, whereas the "g" sites received + charged residues. Furthermore, some Lys residues were changed to Arg to reduce redundancy in the sequence and provide added stability gained from an Arg-Glu salt-bridge interaction. Lastly, using a genetic repacking algorithm, the hydrophobic residues at the "a" and "d" positions were altered to include various nonpolar residues such Ala, Val, Ile, Leu, and Phe residues. The native-like property of α_3C was characterized in tandem with α_3B, and it was demonstrated to exhibit thermodynamic and spectroscopic properties of a well-defined and folded protein.

2.3 Solution Structure of α_3D, the Final Iteration in the THB Design

DeGrado's and coworkers' work had a significant impact on the field of *de novo* protein design through the design, preparation, and characterization of α_3D, a 73-residue peptide with a single conformation in solution and a unique native-like fold.[9] Its well-packed core and

Israel Journal of Chemistry

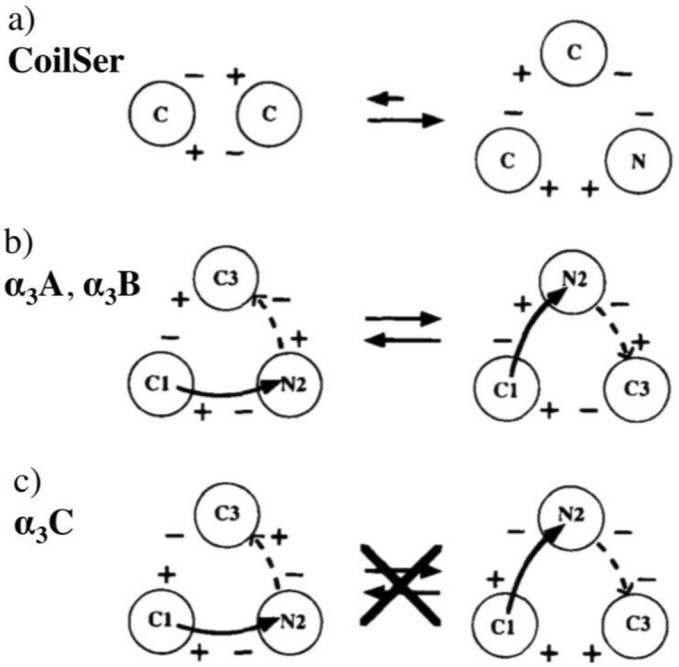

Figure 4. a) Carton scheme representing interhelical electrostatic interactions between α-helices. The circles symbolize α-helices and are illustrated from either the N- or C-terminal end. The numbers correspond to their sequential positions in the THB. The "−" signs denote negatively charged Glu residues in either the "e" or "g" positions, while "+" signs indicate positively charged Lys and Arg residues at the same positions. Solid and dashed lines represent loops that connect helices. a) CS was designed to form a parallel dimer; instead it was observed to pack into an antiparallel trimer with unfavorable interactions with like charges. b) In α_3A and α_3B, the arrangement of the interhelical electrostatic interactions allow for both topologies to be possible. c) The clockwise form was destabilized by careful placement of charged residues at the "e" and "g" positions. In helix 1, only positively (+) charged residues were placed both at the "e" and "g" positions; while in helix 3, negatively (−) charged residues were assigned in those corresponding sites. For helix 2, the "e" sites were given only − charged residues, whereas the "g" sites received + charged residues. Reprinted with permission from Ref [41]. Copyright 1998 The Protein Society.

single topology led to a solution structure; at the time, this was a very challenging feat to achieve (Figure 5). In contrast to its predecessors (α_3A, α_3B, and α_3C), which were chemically synthesized, Walsh *et al.* expressed α_3D in *E. coli*. Met1, Gly2, Gln9, Thr16, and Asp65 were changed in α_3C to generate the sequence of α_3D (Table 2). Thermodynamic studies (chemical and thermal denaturation) showed a scaffold that is fully folded at room temperature (pH 3–7), with a melting temperature (T_m) in the range 80–95 °C, heat capacity (ΔC_p) of 10–12 cal mol^{-1} K^{-1} per residue, Gibbs free energy of unfolding (ΔG_U) of 5.1 kcal mol^{-1}, and an enthalpy (ΔH_{DSC}) value of −44 kcal mol^{-1}.

The solution structure of α_3D was obtained from several three-dimensional (triple resonance, TOCSY, and NOESY) NMR experiments at pH 5.5. About 1260 experimental restraints were used in solving the structure, which comprises of 1191 distances and 69 dihedral angles (φ and χ_1). The ensemble of 13 structures demonstrate a high quality structure, with RMSD values of 1.06, 0.75, and 1.61 Å for the backbone atoms (residues 1–73, N, C^α, C), the backbone atoms in the structure regions (residues 4–21, 24–45, 51–70, N, C^α, C), and the heavy atoms (residues 1–73), respectively. The helical bundle adopts a counterclockwise topology, which is confirmed by the interhelical tilt angles of the lowest energy structure ($\Omega_{1,2}$ = −165°, $\Omega_{1,3}$ = 17° and $\Omega_{2,3}$ = −171°). Further, the χ_1 torsional angles of 14 core residues assumed a single conformation in the ensemble, demonstrating a well-packed apolar core. Ultimately, the success of α_3D demonstrates that the *de novo* design strategy could now serve as a practical method in constructing complex and multistranded scaffolds from a single sequence.

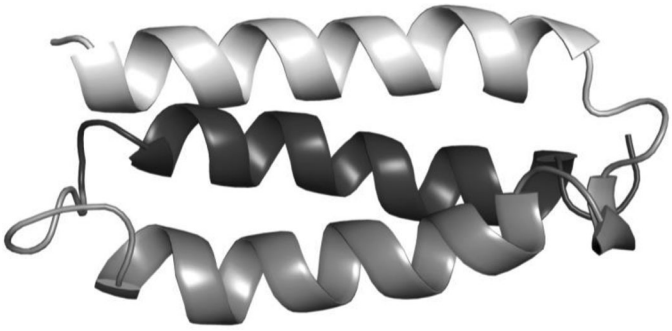

Figure 5. Solution structure of α_3D (PDB code 2A3D) demonstrating a THB fold.[9]

Furthermore, additional solution studies revealed that the backbone ^{15}N and ^{13}C atoms are well-ordered, with restrictive motion on the pico- to nanosecond scale,[42] relative hydration of the backbone amides,[43] and a folding time scale for α_3D in the 1–5 μs range.[44] In addition, mutation studies showed that replacing Ala60 with a Leu or an Ile resulted in 1.5 kcal mol^{-1} net gain in stability.[45]

3. Functionalizing α_3D Framework

3.1. Construction and Structure of a Symmetric Heavy Metal Binding Peptide

α_3D offers a novel opportunity to add function to a well-defined *de novo* designed scaffold (Figure 6a). We redesigned the sequence of α_3D by introducing a tris(cysteine) motif to emulate the type of MS_3 environments that have been proposed for the metalloregulatory proteins MerR,[46–48] ArsR/SmtB,[49] and CadC/CmtR[49–51] (an MS_4 or MS_3O environment). At the C-terminal end of the bundle, three Leu residues at positions 18, 28, and 67 are inside a "hydrophobic box" which is formed by Ile14, Leu21, Phe31, Ile63, and Tyr70. Chakraborty *et al.* functionalized α_3D by mutating the "a" site Leu residues to Cys (Leu18Cys, Leu28Cys, and Leu67Cys) to produce

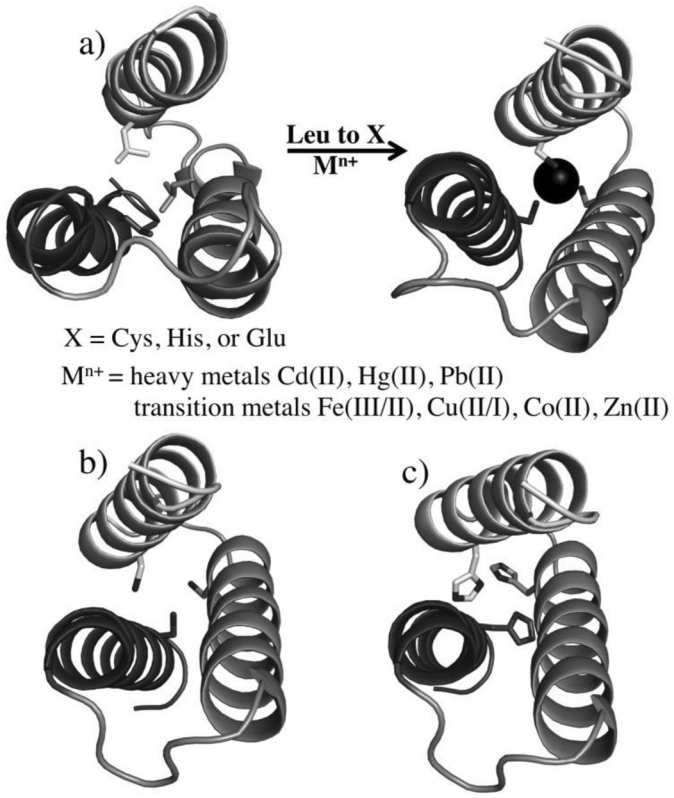

Figure 6. a) Schematic representation of designing a metal center in the α_3D scaffold. b) Top-down view of the tris(cysteine) site in α_3D**IV** modeled from the α_3D structure. c) Top-down view of the tris(histidine) site in α_3D**H$_3$** modeled from the α_3D structure.

α_3D**IV** (Figure 6b).[10] This forms a metal-binding site with two "a" Sγ ligands and one pseudo "a" site at the 28th position in the antiparallel strand.

We recently solved the apo structure of α_3D**IV** at pH 7.0 (unpublished work) to investigate the effects of a Leu to Cys mutation and the preorganization of the tris(cysteine) site prior to metal binding. Like the parent structure α_3D, the three-helix bundle of α_3D**IV** adopts a counterclockwise topology with similar interhelical tilt angles. The structure shows that the tris(cysteine) metal-binding site can easily accommodate heavy metals like Cd(II), Hg(II), and Pb(II), with the 20 lowest energy conformations of the three Cys residues showing great uniformity, indicating a rigid structure. The structure of α_3D**IV** illustrates that we were successful in carving out a metal-binding site within α_3D without significantly compromising its overall structure or stability.

3.2. Characterizing Heavy Metal Binding Properties of α_3DIV

Chakraborty *et al.* determined, via circular dichroism studies, that apo α_3D**IV** is well-folded in solution in the range pH 6–9 and has a chemically-induced ΔG_U of 2.5 kcal mol^{-1}.[10] This ΔG_U is half of the reported value for α_3D, exhibiting a loss in stability after the removal of the packing Leu residues. α_3D**IV** stoichiometrically binds Hg(II), Pb(II), and Cd(II) in a pH-dependent manner. The tris(cysteine) site forms a linear $[Hg(II)S_2(SH)]$ complex below pH 6.0 and a trigonal $[Hg(II)S_3]^-$ complex above pH 8.5; a mixture of both species were observed under intermediate pH conditions (~pH 7.5). Above pH 5.0, Pb(II) and Cd(II) bound α_3D**IV** to generate trigonal pyramidal $[Pb(II)S_3]^-$ and pseudo-tetrahedral $[Cd(II)S_3(N/O)]^-$ geometry, respectively. These coordination modes were determined using various spectroscopic methods and were compared with the physical properties of 3SCC analogues (Table 3). The absorption features of all three metallated species were characterized via UV/Vis spectroscopy. ^{113}Cd and ^{199}Hg NMR, and ^{111m}Cd and ^{199m}Hg perturbed angular correlation spectroscopy (PAC) spectra were obtained for Cd(II)- and Hg(II)-α_3D**IV** to confirm their binding modes in solution. These NMR[52,53] techniques allow us to study the coordination environment at the millisecond timescale, while the PAC[54] techniques can further confirm and elucidate speciation behavior at the micro- to nanosecond timescale. The chemical shift environments of ^{113}Cd and ^{199}Hg NMR are especially sensitive to the coordination environment. The combination of metal NMR and PAC provides a powerful tool in identifying the primary ligand environment, as well additional coordinating ligands, such as solvent molecules or residues that are several layers removed. Furthermore, we have significantly advanced the development of ^{207}Pb NMR,[33,38] using our TRI and CS peptides, by proving how extremely sensitive this nucleus is to subtle changes in the apolar layer above the $Pb(II)S_3$ complex, with a chemical shift range of 5800–5500 ppm.

The ligand-to-metal charge transfer (LMCT) bands of metallated α_3D**IV**[10] in the UV/Vis studies exhibited metal-thiolate transitions comparable with the reported values for its TRI counterparts (Table 3). The Cd(II)-α_3D**IV** species has a λ_{max} at 232 nm (18, 200 M^{-1}cm^{-1}) and Pb(II)-α_3D**IV** exhibits four absorption bands, with a λ_{max} at 236 nm (18,000 M^{-1}cm^{-1}) and a characteristic band at 346 nm (3150 M^{-1}cm^{-1}). The trigonal complex that forms in Hg(II)-α_3D**IV** demonstrates three bands, with a λ_{max} at 247 nm (12,500 M^{-1}cm^{-1}), while the linear species contains one λ_{max} at 240 nm (850 M^{-1}cm^{-1}). From further UV/Vis work, the $[Pb(II)S_3]^-$ complex was determined to have a lower limit binding constant of 2.0×10^7 M^{-1}, while the $[Cd(II)S_3(N/O)]^-$ complex had a lower limit value of 3.1×10^7 M^{-1}.

The linear complex of ^{199}Hg(II)-α_3D**IV** has a chemical shift of −938 ppm, whereas the trigonal form experiences a downfield shift to −244 ppm. The ^{199}Hg NMR spectrum, at an intermediate pH (7.5), contains both the linear and trigonal planar species. The ^{199m}Hg-α_3D**IV** spectra from the PAC analysis confirm this pH-dependent speciation behavior (Figure 7). The PAC parameter, ν_Q, was determined to be 1.48(2) and 1.11(2) GHz for the linear and trigonal complex, respectively, which matches well with

Table 3. Physical parameters of metallated α_3D**IV** compared to 3SCC constructs.[a]

Complex	λ [nm] (Δε [M^{-1} cm^{-1}])	δ (ppm) ^{113}Cd	^{199}Hg	^{207}Pb	ω_0 (rad/ns), η ^{111m}Cd PAC	ν_Q(GHz), η ^{199m}Hg PAC	ref
		583			0.350(6), 0.00(1)[b]		[10]
Cd(α_3D**IV**)	232 (18 200)	595			0.268(4), 0.18(7)[c]		
					0.170(2), 0.50(2)[d]		
Hg(α_3D**IV**)							[10]
3-coordinate	247 (12 500), 265 (8400), 295 (3900)		−244			1.11(2), 0.40(3)	
2-coordinate	240 (850)		−938			1.48(2), 0.15(5)	
Pb(α_3D**IV**)	236 (18 000), 260 (14 400), 278 (9100), 346 (3150)						[10]
Cd(TRIL12C)$_3$	231 (20 600)	619			0.233(8), 0.25(12)		[19]
					0.468(9), 0.12(10)		
Cd(TRIL16C)$_3$	232 (22 600)	625			0.337(2), 0.23(2)		[19]
					0.438(4), 0.20(3)		
Hg(TRIL9C)$_3$			−185		1.164(5), 0.25(2)		[23]
Hg(TRIL9C)$_2$			−908		1.558(7), 0.23(1)		[23]
Hg(TRIL19C)$_3$	230 (21 300), 247 (15 000), 297 (5500)		−316				[23, 25]
Hg(TRIL16C)$_3$	247 (16 800), 265 (10 600), 295 (5000)		−179				[16]
Hg(TRIL16C)$_2$	240 (2700)		−834				[16]
Pb(TRIL12C)$_3$	238 (17 000), 278 (12 300), 343 (3700)			5814[e]			[21, 33]
Pb(TRIL16C)$_3$	236 (18 500), 260 (16 500), 278 (14 500), 346 (3400)			5612[f]			[21, 33]

[a] UV/Vis, metal (^{113}Cd, ^{199}Hg and ^{207}Pb) NMR and (^{111m}Cd and ^{199m}Hg) PAC. L9C and L16C are "a" site constructs, while L12C and L19C are "d" sites. [b] CdS_3O in *exo* conformation. [c] CdS_3O in *endo* conformation. [d] CdS_3N species. [e] ^{207}Pb chemical shift for Pb(CSL12C)$_3$; ref 33. [f] ^{207}Pb chemical shift for Pb(CSL16C)$_3$; ref 33.

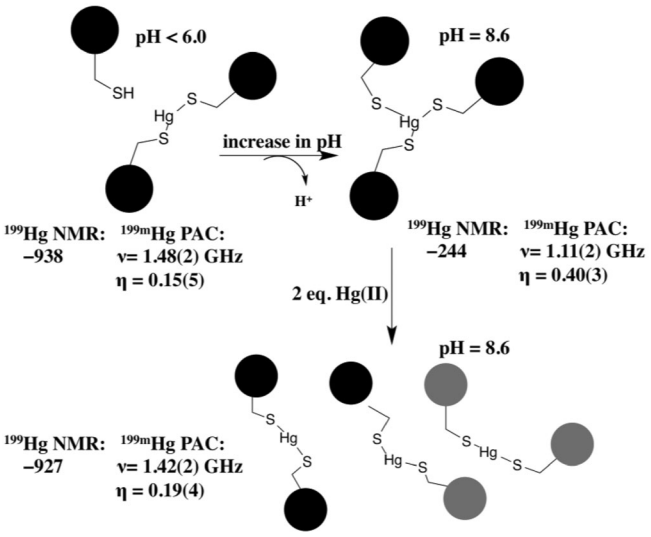

Figure 7. Schematic representation of the pH- and stoichiometric-dependent behavior of Hg(II) species in α_3D**IV**.[10,55]

the reported ν_Q values for 2- and 3-coordinate Hg(II) in 3SCC constructs.[31] These ν_Q values were also observed at pH 7.5, demonstrating the presence of both linear and trigonal planar species. In hindsight, these results show that we have created a peptide scaffold that can finely control the coordination environment of Hg(II) ions. Additionally, Chakraborty *et al.* observed that the addition of 2 equivalents of Hg(II) induced the formation of a dimer species, where Hg(II) atoms bridge two peptides through a linear complex.[55] This dimer species was confirmed with both ^{199}Hg(II) NMR and ^{199m}Hg(II) PAC.

The ^{113}Cd NMR spectrum of ^{113}Cd-α_3D**IV** shows overlapping resonance peaks at 583 and 595 ppm. Based on these chemical shift positions, this result indicates the presence of two 4-coordinate Cd(II) species. ^{111m}Cd PAC was again collected to supplement the ^{113}Cd NMR result, but in this case, it was used to define the two species observed in the NMR time scale. The ^{111m}Cd PAC showed three nuclear quadrupole interactions at 0.35, 0.27, and 0.17 rad ns^{-1}. The peaks at 0.35 and 0.27 rad ns^{-1} agree well with a CdS_3O complex with two conformations, *endo* and *exo*. The frequency value at 0.17 rad ns^{-1} fitted well with CdS_3N species, where the N ligand was proposed to originate from the imidazole ring of His72. Overall, not only did the combination of metal NMR and PAC provide a way to accurately characterize our *de novo* designed peptides, it also gave powerful insights into how toxic heavy metals may interact with native proteins.

3.3. Constructing a Symmetric Metalloenzyme Site in α_3D

Our work with α_3D was further expanded to incorporate a tris(histidine) metal-binding site reminiscent of carbonic anhydrase (Figure 6c). This metalloenzyme plays a vital role in respiration, vision, cancer metathesis, regulation of acid-base equilibria, and other processes in animals, plants, and bacteria. Human carbonic anhydrase II is one of the most efficient enzymes (approaching the diffusion limit) which catalyzes the reversible interconversion between CO_2 and HCO_3^-.[56] Even though the mechanism,

structure, and inhibition have been previously studied, *de novo* protein design still offers a novel approach to study and replicate an important function of a native metalloenzyme in a simplified peptide system. We have previously demonstrated a carbonic anhydrase model in a bimetallic 3SCC construct $[Hg(II)]_S[Zn(II)(H_2O/OH^-)]_N(TRIL9CL23H)_3^{n+}$ and Zastrow *et al.* reported this model to be within 500-fold of the fastest isozyme (CAII), which is the fastest CA model to date (Figure 2a).[27,30] Nevertheless, CAII contains residues that participate in hydrogen-bonding networks, and the self-associating nature of our 3SCC construct limits its use in preparing asymmetric sites. Thus, we remodeled the zinc catalytic site of CA into α_3D to recapitulate CA activity. Now that this is established, we hope to add hydrogen-bonding residues in the second coordination sphere of the Zn(II) complex in future CA designs of α_3D.

Cangelosi *et al.* incorporated a tris(histidine) site in α_3D to yield α_3D**H$_3$** (Figure 6c), a *de novo* designed metalloenzyme model that exhibited CA activity.[11] The sequence of α_3D**H$_3$** (Table 2) was expanded by four residues (77 in α_3D**H$_3$**), which led to a peptide with increased yields during expression, from ~100 to 230 mg L^{-1}. His residues were substituted at positions 18, 28, and 67, and a His72Val mutation was also incorporated to eliminate a competing ligand. At pH 9.0, the apo form folds well in solution (82% folded), according to the 208 and 222 nm bands that were observed in the CD spectrum, and has a chemically induced ΔG_U of 3.1 kcal mol^{-1}. The Zn(II)-α_3D**H$_3$** complex was characterized using UV/Vis and X-ray absorption spectroscopies, while its CA activity was determined with Khalifah's stopped-flow indicator technique.[57]

Using a UV/Vis Zincon colorimetric assay,[58] the apparent Zn(II) binding constant to α_3D**H$_3$** was determined to be 150 ± 40 nM at pH 7.5 and it strengthened to 59 ± 9 nM at pH 9.0. When compared with CA, these affinity values are only two orders of magnitude weaker than the recent value determined for CAII (0.45 nM),[56] and stronger than the $[Hg(II)]_S[Zn(II)(H_2O/OH^-)]_N(TRIL9CL23H)_3^{n+}$ (0.8 ± 0.1 μM at pH 7.5 and 0.22 ± 0.06 μM at pH 9.0)[30] CA model. From extended X-ray absorption fine structure spectroscopy, the Zn(II)-α_3D**H$_3$** coordination environment (at pH 9.0) fitted well to a site that contains 1 oxygen (from an exogenous H_2O or OH molecule) and 3 nitrogen atoms from each His residue bound to a Zn(II) atom at 1.90 and 1.99 Å, which matches well with the Zn complex in CAII with a Zn–N/O bond length of 1.98 Å (pH 7.0).[56]

To demonstrate the success of α_3D**H$_3$** as a metalloenzyme, Cangelosi *et al.* performed a stopped-flow CO_2 hydration assay using Khalifah's indicator technique. The maximal catalytic efficiency (k_{cat}/K_M), which was derived from the k_{cat}/K_M values for pH 8–9.5, and the kinetic pK_a for the deprotonation of Zn(II)-bound water to yield the active $[Zn(II)N_3O]^{1+}$ hydroxide complex were calculated to be 6.9×10^4 L mol^{-1} s^{-1} and 9.4, respectively. When compared with two small molecule models, Zn(II)(tris(4,5-di-*n*-propyl-2-imidazolyl)-phosphine)[59] and Zn(II)nitrilotris(2-benzimidazolylmethyl-6-sulfonate),[60] which both have a $Zn(II)N_3O$ complex and show CA activity, Zn(II)-α_3D**H$_3$** significantly outperformed these models, exhibiting a second-order rate constant (k_2) that was 14-fold higher. The CO_2 hydration efficiency of Zn(II)-α_3D**H$_3$** is 2.6-fold slower than its 3SCC counterpart,[27] 1400-fold less efficient than CAII,[61] but only 11-fold slower than CAIII.[62] The decrease in the catalytic activity, as compared with our 3SCC CA model, could be as a result of a weaker dipole, less-symmetric environment for the imidazole rings, and difference in the electrostatics at the metal-binding site in the antiparallel bundle of α_3D**H$_3$**. Furthermore, a product inhibition assay was performed on Zn(II)-α_3D**H$_3$**, using acetate, since it serves as a more probable mimic of bicarbonate. At pH 8.5, the first-order rate constant (k_{cat}) experienced a modest decrease from 82 ± 6 to 66 ± 4 s^{-1}. This inhibition result indicates no significant loss in catalytic activity, and illustrates a CA model capable of preventing product inhibition, which is a major problem in small molecule models of enzymes. Overall, our work on Zn(II)-α_3D**H$_3$** exhibits that we are successful in recapitulating the primary active site and the function of carbonic anhydrase in a simplified antiparallel THB scaffold, a metalloenzyme that is found in a twisted β-sheet fold in nature.

4. Future Designs

4.1. Redesign of α_3DIV to Improve Metal Binding

The structure of α_3D**IV** demonstrates that we are still able to retain a well-folded peptide construct, even after mutating the core packing Leu to Cys residues to achieve a thiol-rich metal-binding site. With this knowledge, we can now attempt to prepare an antiparallel three-helix bundle construct (via modeling) that will contain a more preformed or more symmetric tris(cysteine) metal-binding site which resembles "a" site ligands. When overlaying the 20 lowest structures of α_3D**IV**, we observed that the Sγ of Cys28 consistently points towards the C-terminal end, forming a skewed S3 plane. Thus, the first iteration involves rearranging the Cys28 by one layer towards the N-terminal end. This modification requires Cys28Phe and Phe31Cys mutations (Figure 8a). Along with Cys18 and Cys67, a Cys in the 31st position could produce an S3 plane which is more perpendicular to the helical bundle than the current α_3D**IV** construct. The Phe in the 28th position could provide a hydrophobic capping interaction that forces Cys31 to take an "a" site orientation. We are currently working on these modifications and plan to characterize the heavy metal binding properties of this new α_3D construct fully.

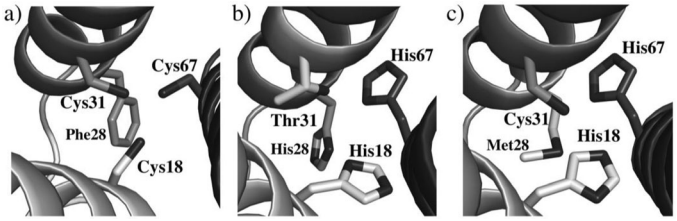

Figure 8. Future α_3D designs. a) α_3D**IV** Cys28Phe/Phe31Cys mutant designed to achieve a more symmetric tris(cysteine) site. b) α_3D**H$_3$** Phe31Thr construct, where the Thr could serve as a hydrogen-bonding residue and lower the deprotonation pK_a of the water molecule bound to the ZnN_3 center. c) Asymmetric 2His, Cys and Met cupredoxin incorporated in the α_3D scaffold.

4.2. Redesign of α_3DH$_3$ to Improve Catalytic Activity

The crystal structure of Human CAII revealed that Zn(II) is coordinated to three His residues and a water molecule/hydroxide ion.[12,39] In addition, this structure exposed an elaborate H-bonding network, facilitated by Thr, Asn, and Gln residues in the second coordination sphere. Thr199 forms an H-bonding interaction with the hydroxide nucleophile of the Zn(II) center, which was determined to be significant for the acid-base catalysis activity of CA. Mutation studies of this residue resulted in a 1.5–2.5 unit increase in the pK_a (from 6.8) of the H_2O molecule to the OH^- active form, resulting in 100-fold loss in catalytic activity.[12,39,63] Our current CA constructs Zn(II)-α_3D**H$_3$** and $[Hg(II)]_5[Zn(II)(H_2O/OH^-)]_N(TRIL9CL23H)_3^{n+}$ have pK_a values for this deprotonation process 2–2.6 units higher, and demonstrate CO_2 hydration activities that are 500–1400-fold less efficient than CAII.[11,27,30,61] Nevertheless, both constructs only contain the primary coordination sphere ($ZnHis_3$) and do not contain H-bonding interactions that greatly enhance CA activity. Consequently, to achieve native-like efficiency, we now have to consider incorporating secondary interactions in our designs. Since our 3SCC analogues are not ideal for adding H-bonding residues inside the core in a step-wise manner, we must turn to our α_3D**H$_3$** to design future CA models which investigate essential secondary interactions (as demonstrated in Figure 8b).

4.3. Design of an Electron-transfer Site in α_3D

Cupredoxins are copper-containing proteins that shuttle electrons between two-membrane-bound proteins in photosynthesis, and for this reason, have been extensively studied to understand their fundamental function in nature.[64] The copper ion is coordinated to a well-defined and pre-organized asymmetric metal-binding site encapsulated by a β-barrel fold. It contains two histidines, one cysteine, and one or two more weakly bound residues to form a 3- to 5-coordinate copper complex. The rack-induced bonding model has been used to describe the copper site in these cupredoxins, which states that the ligand environment in a β-barrel fold forces the copper ion, regardless of the oxidation state, into a strict geometry.[65] This feature alone makes cupredoxins an ideal candidate for *de novo* design.

The most successful *de novo* designed model that demonstrates the spectroscopic properties of cupredoxins was achieved in a parallel four-stranded coiled-coil.[66] Therefore, α_3D offers a viable framework in achieving an asymmetric cupredoxin site. Now knowing that we can incorporate cysteine ligands in α_3D**IV** and bulky His residues in α_3D**H$_3$**, we have designed several constructs (Figure 8c) to test the importance of the β-barrel fold in copper ET proteins (unpublished work). Ultimately, these designed constructs will provide a novel approach for investigating biological long-range electron transfer.

5. Summary and Outlook

De novo protein design is a biologically relevant approach used to understand the structure-function relationship in the metal centers of native proteins, and is quickly becoming a viable method for developing heretofore unknown protein folds with nature-inspired metal-binding sites. As we have discussed herein, the field of *de novo* metalloproteins and enzymology has made great advances over the past decade and promises the future capability of preparing multicenter redox enzymes designed from first principles. At present, well-defined and well-folded scaffolds have been made available for helical bundle motifs,[67–70] with the α_3D system being an excellent example. Here, we have demonstrated that it is possible to functionalize the α_3D scaffold to generate structural and catalytic sites, while studies are ongoing to generate electron-transfer centers within the same fold. We and others intend to build upon this work, constructing nature-inspired asymmetric metal-binding sites that form the foundation for future designs of artificial metalloenzymes and metalloproteins, which not only mimic natural reactions, but also confer new catalytic processes, ranging from CO_2 and H^+ reduction to water oxidation and fine chemical synthesis.

Acknowledgements

J. S. P. and V. L. P. would like to thank the National Institutes of Health (NIH) for financial support (ES012236).

References

[1] K. J. Waldron, J. C. Rutherford, D. Ford, N. J. Robinson, *Nature* **2009**, *460*, 823–830.
[2] Y. Lu, S. M. Berry, T. D. Pfister, *Chem. Rev.* **2001**, *101*, 3047–3080.

[3] Y. Lu, N. Yeung, N. Sieracki, N. M. Marshall, *Nature* **2009**, *460*, 855–862.
[4] F. Yu, V. M. Cangelosi, M. L. Zastrow, M. Tegoni, J. S. Plegaria, A. G. Tebo, C. S. Mocny, L. Ruckthong, H. Qayyum, V. L. Pecoraro, *Chem. Rev.* **2014**, *114*, 3495–3578.
[5] M. L. Zastrow, V. L. Pecoraro, *Coord. Chem. Rev.* **2013**, *257*, 2565–2588.
[6] W. F. DeGrado, C. M. Summa, V. Pavone, F. Nastri, A. Lombardi, *Annu. Rev. Biochem.* **1999**, *68*, 779–819.
[7] D. Ghosh, V. L. Pecoraro, *Curr. Opin. Chem. Biol.* **2005**, *9*, 97–103.
[8] D. P. Giedroc, A. I. Arunkumar, *Dalton Trans.* **2007**, 3107–3120.
[9] S. T. R. Walsh, H. Cheng, J. W. Bryson, H. Roder, W. F. DeGrado, *Proc. Natl. Acad. Sci. U.S.A.* **1999**, *96*, 5486–5491.
[10] S. Chakraborty, J. Yudenfreund-Kravitz, P. W. Thulstrup, L. Hemmingsen, W. F. DeGrado, V. L. Pecoraro, *Angew. Chem. Int. Ed.* **2011**, *50*, 2049–2053.
[11] V. M. Cangelosi, A. Deb, J. E. Penner-Hahn, V. L. Pecoraro, *Angew. Chem. Int. Ed.* **2014**, *53*, 7900–7903.
[12] J. F. Krebs, J. A. Ippolito, D. W. Christianson, C. A. Fierke, *J. Biol. Chem.* **1993**, *268*, 27458–27466.
[13] J. M. Guss, H. D. Bartunik, H. C. Freeman, *Acta Crystallogr. Sect. B: Struct. Sci.* **1992**, *48*, 790–811.
[14] A. F. A. Peacock, O. Iranzo, V. L. Pecoraro, *Dalton Trans.* **2009**, 2271–2280.
[15] D. Ghosh, V. L. Pecoraro, *Inorg. Chem.* **2004**, *43*, 7902–7915.
[16] G. R. Dieckmann, D. K. McRorie, D. L. Tierney, L. M. Utschig, C. P. Singer, T. V. O'Halloran, J. E. Penner-Hahn, W. F. DeGrado, V. L. Pecoraro, *J. Am. Chem. Soc.* **1997**, *119*, 6195–6196.
[17] G. R. Dieckmann, D. K. McRorie, J. D. Lear, K. A. Sharp, W. F. DeGrado, V. L. Pecoraro, *J. Mol. Biol.* **1998**, *280*, 897–912.
[18] B. T. Farrer, N. P. Harris, K. E. Balchus, V. L. Pecoraro, *Biochemistry* **2001**, *40*, 14696–14705.
[19] M. Matzapetakis, B. T. Farrer, T.-C. Weng, L. Hemmingsen, J. E. Penner-Hahn, V. L. Pecoraro, *J. Am. Chem. Soc.* **2002**, *124*, 8042–8054.
[20] K. H. Lee, M. Matzapetakis, S. Mitra, E. N. Marsh, V. L. Pecoraro, *J. Am. Chem. Soc.* **2004**, *126*, 9178–9179.
[21] M. Matzapetakis, D. Ghosh, T. C. Weng, J. E. Penner-Hahn, V. L. Pecoraro, *J. Biol. Inorg. Chem.* **2006**, *11*, 876–890.
[22] O. Iranzo, D. Ghosh, V. L. Pecoraro, *Inorg. Chem.* **2006**, *45*, 9959–9973.
[23] O. Iranzo, P. W. Thulstrup, S. Ryu, L. Hemmingsen, V. L. Pecoraro, *Chem. Eur. J.* **2007**, *13*, 9178–9190.
[24] O. Iranzo, C. Cabello, V. L. Pecoraro, *Angew. Chem. Int. Ed.* **2007**, *46*, 6688–6691.
[25] M. Łuczkowski, M. Stachura, V. Schirf, B. Demeler, L. Hemmingsen, V. L. Pecoraro, *Inorg. Chem.* **2008**, *47*, 10875–88.
[26] A. F. A. Peacock, L. Hemmingsen, V. L. Pecoraro, *Proc. Natl. Acad. Sci. U.S.A.* **2008**, *105*, 16566–16571.
[27] M. L. Zastrow, A. F. A. Peacock, J. A. Stuckey, V. L. Pecoraro, *Nat. Chem.* **2011**, *4*, 118–123.
[28] G. Zampella, K. P. Neupane, L. De Gioia, V. L. Pecoraro, *Chem. Eur. J.* **2012**, *18*, 2040–2050.
[29] M. Tegoni, F. Yu, M. Bersellini, J. E. Penner-Hahn, V. L. Pecoraro, *Proc. Natl. Acad. Sci. U.S.A.* **2012**, *109*, 21234–21239.
[30] M. L. Zastrow, V. L. Pecoraro, *J. Am. Chem. Soc.* **2013**, *135*, 5895–5903.
[31] F. Yu, J. E. Penner-Hahn, V. L. Pecoraro, *J. Am. Chem. Soc.* **2013**, *135*, 18096–18107.
[32] O. Iranzo, S. Chakraborty, L. Hemmingsen, V. L. Pecoraro, *J. Am. Chem. Soc.* **2011**, *133*, 239–251.
[33] K. P. Neupane, V. L. Pecoraro, *Angew. Chem. Int. Ed.* **2010**, *49*, 8177–8180.
[34] B. T. Farrer, V. L. Pecoraro, *Proc. Natl. Acad. Sci. U.S.A.* **2003**, *100*, 3760–3765.
[35] D. S. Touw, C. E. Nordman, J. A. Stuckey, V. L. Pecoraro, *Proc. Natl. Acad. Sci. U.S.A.* **2007**, *104*, 11969–11974.
[36] A. F. A. Peacock, J. A. Stuckey, V. L. Pecoraro, *Angew. Chem. Int. Ed.* **2009**, *48*, 7371–7374.
[37] S. Chakraborty, D. S. Touw, A. F. A. Peacock, J. A. Stuckey, V. L. Pecoraro, *J. Am. Chem. Soc.* **2010**, *132*, 13240–13250.
[38] K. P. Neupane, V. L. Pecoraro, *J. Inorg. Biochem.* **2011**, *105*, 1030–1034.
[39] B. S. Avvaru, C. U. Kim, K. H. Sippel, S. M. Gruner, M. Agbandje-McKenna, D. N. Silverman, R. McKenna, *Biochemistry* **2010**, *49*, 249–251.
[40] B. Lovejoy, S. Choe, D. Cascio, D. K. McRorie, W. F. DeGrado, D. Eisenberg, *Science* **1993**, *259*, 1288–1293.
[41] J. W. Bryson, J. R. Desjarlais, T. M. Handel, W. F. DeGrado, *Protein Sci.* **1998**, *7*, 1404–1414.
[42] S. T. R. Walsh, A. L. Lee, W. F. DeGrado, A. J. Wand, *Biochemistry* **2001**, *40*, 9560–9569.
[43] S. T. R. Walsh, R. P. Cheng, W. W. Wright, D. O. V. Alonso, V. Daggett, J. M. Vanderkooi, W. F. DeGrado, *Protein Sci.* **2003**, *12*, 520–531.
[44] Y. Zhu, D. O. V. Alonso, K. Maki, C.-Y. Huang, S. J. Lahr, V. Daggett, H. Roder, W. F. DeGrado, F. Gai, *Proc. Natl. Acad. Sci. U.S.A.* **2003**, *100*, 15486–15491.
[45] S. T. R. Walsh, V. I. Sukharev, S. F. Betz, N. L. Vekshin, W. F. DeGrado, *J. Mol. Biol.* **2001**, *305*, 361–373.
[46] T. V. O'Halloran, C. Walsh, *Science* **1987**, *235*, 211–214.
[47] J. G. Wright, M. J. Natan, F. M. MacDonnel, D. M. Ralston, T. V. O'Halloran, *Prog. Inorg. Chem.* **1990**, *38*, 323–412.
[48] J. G. Wright, H. T. Tsang, J. E. Penner-Hahn, T. V. O'Halloran, *J. Am. Chem. Soc.* **1990**, *112*, 2434–2435.
[49] L. S. Busenlehner, T. C. Weng, J. E. Penner-Hahn, D. P. Giedroc, *J. Mol. Biol.* **2002**, *319*, 685–701.
[50] J. Ye, A. Kandegedara, P. Martin, B. P. Rosen, *J. Bacteriol.* **2005**, *187*, 4214–4221.
[51] L. Banci, I. Bertini, F. Cantini, S. Ciofi-Baffoni, J. S. Cavet, C. Dennison, A. I. Graham, D. R. Harvie, N. J. Robinson, *J. Biol. Chem.* **2007**, *282*, 30181–30188.
[52] G. Öz, D. L. Pountney, I. M. Armitage, *Biochem. Cell Biol.* **1998**, *76*, 223–234.
[53] I. Armitage, T. Drakenberg, B. Reilly, *Met. Ions Life Sci.* **2013**, *11*, 117–144.
[54] L. Hemmingsen, M. Stachura, P. W. Thulstrup, N. J. Christensen, K. Johnston, *Hyperfine Interact.* **2010**, *197*, 255–267.
[55] S. Chakraborty, PhD thesis, University of Michigan (USA), **2011**.
[56] H. Song, D. L. Wilson, E. R. Farquhar, E. A. Lewis, J. P. Emerson, *Inorg. Chem.* **2012**, *51*, 11098–11105.
[57] R. G. Khalifah, *J. Biol. Chem.* **1971**, *246*, 2561–2573.
[58] R. M. Rush, J. H. Yoe, *Anal. Chem.* **1954**, *26*, 1345–1347.
[59] H. Slebocka-Tilk, J. L. Cocho, Z. Frakman, R. S. Brown, *J. Am. Chem. Soc.* **1984**, *106*, 2421–2431.
[60] K. Nakata, N. Shimomura, N. Shiina, M. Izumi, K. Ichikawa, M. Shiro, *J. Inorg. Biochem.* **2002**, *89*, 255–266.
[61] J. E. Jackman, K. M. Merz Jr, C. A. Fierke, *Biochemistry* **1996**, *35*, 16421–16428.

[62] D. A. Jewell, C. Tu, S. R. Paranawithana, S. M. Tanhauser, P. V. LoGrasso, P. J. Laipis, D. N. Silverman, *Biochemistry* **1991**, *30*, 1484–1490.
[63] Z. Liang, Y. Xue, G. Behravan, B.-H. Jonsson, S. Lindskog, *Eur. J. Biochem.* **1993**, *211*, 821–827.
[64] E. I. Solomon, R. K. Szilagyi, S. DeBeer George, L. Basumallick, *Chem. Rev.* **2004**, *104*, 419–458.
[65] B. G. Malmström, *FEBS* **1994**, *223*, 711–718.
[66] D. Shiga, D. Nakane, T. Inomata, Y. Funahashi, H. Masuda, A. Kikuchi, M. Oda, M. Noda, S. Uchiyama, K. Fukui, K. Kanaori, K. Tajima, Y. Takano, H. Nakamura, T. Tanaka, *J. Am. Chem. Soc.* **2010**, *132*, 18191–18198.
[67] C. T. Choma, J. D. Lear, M. J. Nelson, P. L. Dutton, D. E. Robertson, W. F. DeGrado, *J. Am. Chem. Soc.* **1994**, *116*, 856–865.
[68] A. Lombardi, C. M. Summa, S. Geremia, L. Randaccio, V. Pavone, W. F. DeGrado, *Proc. Natl. Acad. Sci. U.S.A.* **2000**, *97*, 6298–6305.
[69] J. Zhuang, J. H. Amoroso, R. Kinloch, J. H. Dawson, M. J. Baldwin, B. R. Gibney, *Inorg. Chem.* **2004**, *43*, 8218–8220.
[70] S. S. Huang, R. L. Koder, M. Lewis, A. J. Wand, P. L. Dutton, H. B. Gray, *Proc. Natl. Acad. Sci. U.S.A.* **2004**, *101*, 5536–554.

Received: October 1, 2014
Accepted: November 4, 2014
Published online: January 15, 2015